

Form record received

International Workshop on Waldenstrom's Macroglobulinemia <pattersonkent@outlook.com>

Mon 7/15/2024 4:39 PM

To:Patterson, Christopher <Christopher_Patterson@DFCI.HARVARD.EDU>

External Email - Use Caution

Record saved to database with ID: 154

Form ID: 1

Form title: Abstract Submission

Form name: Abstract_Submission

Submitted at: 2024-07-15 16:38:45

Submitter IP: 170.223.207.85

User-ID: 0

Username: -

User full name: -

Submitter provider: Unknown

Submitter browser: Mozilla/5.0 (Windows NT 10.0; Win64; x64) AppleWebKit/537.36 (KHTML, like Gecko)

Chrome/124.0.0.0 Safari/537.36 Edg/124.0.0.0

Submitter operating system: win

First Name: Hao

Last Name: Sun

Email: HAO_SUN@DFCI.HARVARD.EDU

Phone Number (optional): 4134047994

Registration Type: Delegate

Abstract Title: Single-Cell Marrow Analysis Reveals Abnormal Activation of T Cells and Monocytes, Identifies CD35 as a New Biomarker in Waldenstrom Macroglobulinemia

Select abstract file to attach:

/home/dkwolfpk2016/public_html/waldenstromsworkshop/media/breezingforms/uploads/haosuniwwm12singlecellimmunecd35.docx

Please consider me for a YIA grant: YIA Grant Consideration

Conference: IWWM12

Single-Cell Marrow Analysis Reveals Abnormal Activation of T Cells and Monocytes, Identifies CD35 as a New Biomarker in Waldenstrom Macroglobulinemia

Hao Sun^{1,2,3}, Xia Liu^{1,2}, Maria Luisa Guerrero^{1,2}, Nicholas Tsakmaklis^{1,2}, Amanda Kofides^{1,2}, Andres Felipe Ramirez Gamero¹, Catherine A. Flynn¹, Christopher J. Patterson^{1,2}, Mu Hao³, Lugui Qiu³, Shayna R. Sarosiek^{1,2}, Jorge J. Castillo^{1,2}, Zachary R. Hunter^{1,2}, Shirong Liu^{1,2}, Steven P. Treon^{1,2}

¹ Bing Center for Waldenström Macroglobulinemia, Dana-Farber Cancer Institute, Boston, MA, USA.

² Harvard Medical School, Boston, MA, USA.

³ Institute of Hematology and Blood Diseases Hospital, Chinese Academy of Medical Sciences and Peking Union Medical College, Tianjin, China.

Background:

Waldenström macroglobulinemia (WM) is an indolent B-cell malignancy for which there is currently no cure. The underlying molecular mechanisms and the impact of the immunosuppressive microenvironment on WM oncogenesis remain still incompletely understood.

Methods:

We utilized single-cell RNA sequencing combined with BCR and TCR sequencing to analyze bone marrow samples from 7 healthy donors (HD) and 26 newly diagnosed WM patients. In vitro experiments were performed using antibodies to validate the function of the novel WM biomarker CD35 in BCWM.1 and MWCL-1 cell lines.

Results:

Our findings highlight significant differences in the immune microenvironment between WM patients and healthy donors (**Fig. 1A**). In WM patients, we observed a marked reduction in CD8⁺ naïve T cells and an increase in CD8⁺ effector T cells compared to healthy donors. Monocyte proportions were also lower in WM patients. Several stages of normal B cells, including pre-B cells, naïve B cells, and memory B cells, were significantly reduced in WM patients. Notably, clonal B cells were predominantly found in CXCR4^{mut} patients, while clonal plasma cells were more common in CXCR4^{wt} patients (**Fig. 1B**).

We employed non-negative matrix factorization to characterize T cells and monocytes, identifying key signatures based on their top 10 genes. Four T cell signatures were identified: T-sig1, enriched in CD4⁺ T cells; T-sig2, enriched in CD8⁺ memory and effector T cells; T-sig3, representing the TCR activation pathway and significantly elevated in WM patients; and T-sig4, enriched in CD8⁺ naïve T cells. There were no significant differences in T-sig3 between

CXCR4^{mut} and CXCR4^{wt} patients (Fig. 1C).

By defining T cell exhaustion and cytotoxicity scores, we found a significant reduction in the cytotoxic capacity of CD8⁺ T cells and an increase in exhaustion scores in WM patients, with no significant differences between CXCR4^{mut} and CXCR4^{wt} patients (Fig. 1D). Additionally, four monocyte signatures were identified. M-sig2, associated with cellular activation, was significantly increased in WM patients. M-sig4, enriched for MHC II-related molecules, was significantly reduced in CD14⁺ monocytes, indicating a possible enrichment of CD14⁺HLA-DR^{-low} MDSCs in WM patients. The pro-inflammatory M-sig1 was significantly increased, whereas the anti-inflammatory M-sig3 was significantly decreased in WM patients (Fig. 2A).

To identify new biomarkers for WM tumor cells, we used logistic regression to create a classifier distinguishing WM tumor cell (clonal B cells and clonal plasma cells) from normal counterparts (memory B cells and normal plasma cells) in healthy donors, achieving an AUC of 0.99. This analysis revealed the top 20 differentially expressed genes (DEGs) between tumor and normal cells (Fig. 2B).

Patient-specific transcriptional changes were further discovered by comparing tumor cells to normal cells from the same samples. Among the top 20 DEGs, CR1 (CD35) had the highest AUC for distinguishing tumor cells from normal cells in patients. This finding was validated using an additional bulk-RNA dataset, which showed significantly reduced CD35 expression in WM.

Given the role of CD35 in inhibiting BCR signaling pathways, we treated WM cell lines with CD35 antibodies. The CD35 antibody significantly inhibited tumor cell proliferation, with IC50 values for BCWM.1 cells ranging from 8.34-26.52µg/mL and for MWCL-1 cells from 5.67-12.04µg/mL (Fig. 2C). Flow cytometry demonstrated that CD35 antibodies induced apoptosis in WM tumor cells in a dose-dependent manner (Fig. 2D).

Conclusion:

Our study reveals that T cells and monocytes in the WM bone marrow microenvironment are hyperactivated but exhibit reduced cytotoxic function. We identified CD35 as a robust marker for distinguishing WM tumor cells from normal counterparts in patients. CD35 antibodies induce apoptosis and significantly inhibit the proliferation of WM tumor cells, suggesting CD35 as a promising biomarker and therapeutic target for WM.

Fig. 1

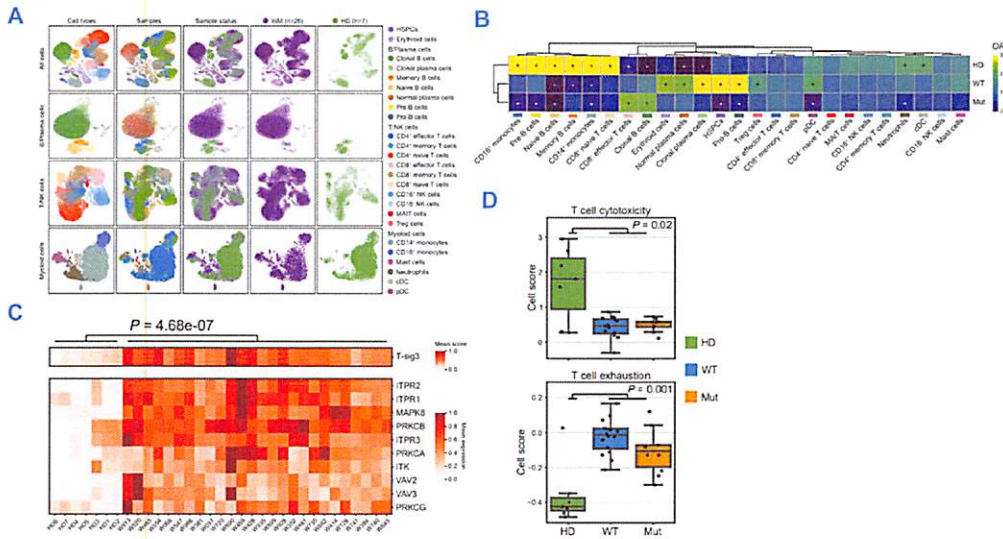


Fig. 1 | Differences in the Immune Microenvironment between WM Patients and Healthy Donors (A) Overview of the annotated cells from newly diagnosed WM patients (n=26) and healthy donors (n=7).

(B) Heatmap illustrating the odds ratios (OR) of each cell type in healthy donors, CXCR4^{mut} WM patients, or CXCR4^{wt} WM patients based on Fisher's exact test. A high OR with an asterisk indicates a cell type more prevalent in the group.

(C) Heatmap showing the mean score of T-sig3 across the samples, including the mean expression of the top 10 genes of T-sig3. Statistical analysis was performed using the Mann-Whitney test.

(D) Boxplot depicting the mean cell score of T cell cytotoxicity and exhaustion in samples from the three groups. Statistical analysis was performed using the Mann-Whitney test.

Fig. 2

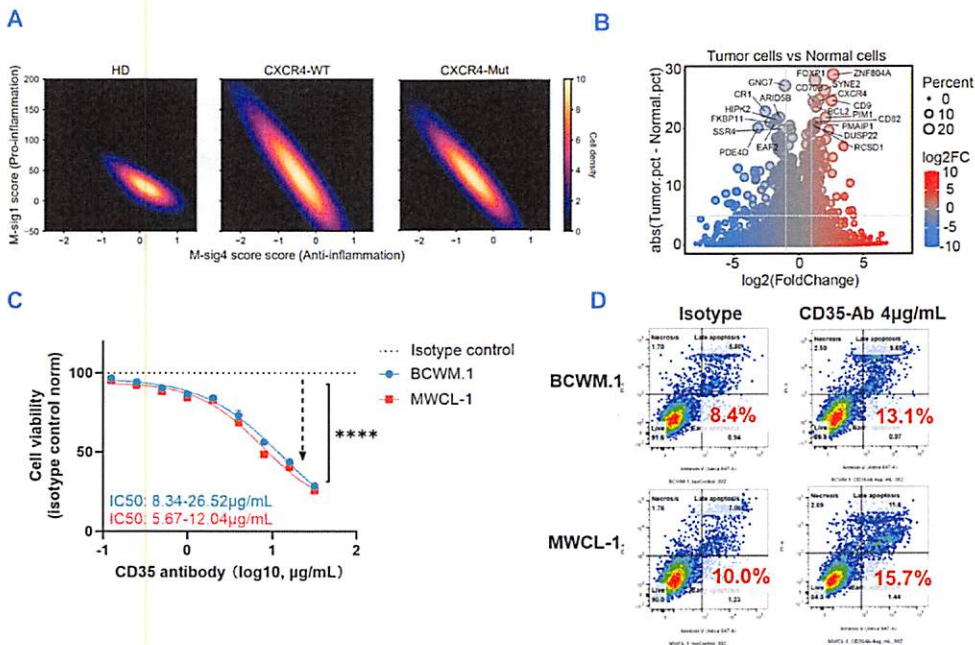


Fig. 2 | Analysis of T cell inflammation and CD35 antibody effects. (A) Flow cytometry plots showing M-sig1 (Pro-inflammation) vs M-sig4 (Anti-inflammation) for HD, CXCR4-WT, and CXCR4-Mut groups. (B) Bubble plot showing log2(FoldChange) vs abs(Tumor.pct - Normal.pct) for tumor vs normal cells. (C) Dose-response curve for CD35 antibody (log10, µg/mL) showing cell viability (isotype control norm) for Isotype control, BCWM.1, and MWCL-1. (D) Flow cytometry plots showing BCWM.1 and MWCL-1 under Isotype and CD35-Ab 4µg/mL conditions, with percentages of cells in the 'Low apoptosis' quadrant.

Fig. 2 | CD35 as a New Biomarker in WM

(A) Fitted density plot illustrating the pro-inflammation and anti-inflammation scores in monocytes from three groups.

(B) Volcano plot showing the differentially expressed genes between WM tumor cells (including clonal B cells and plasma cells) and normal cells (including memory B cells and plasma cells) from healthy donors.

(C) Line plot showing the relative cell viability normalized to the isotype control in the BCWM.1 and MWCL-1 cell lines treated with CD35 antibody. Statistical analysis was performed using one-way ANOVA.

(D) Density dot plots from flow cytometry analysis displaying the apoptosis of BCWM.1 and MWCL-1 cells treated with CD35 antibody.